Response to Editor's comments on acp-2014-431: Biomass burning related ozone damage on vegetation over the Amazon forest: A model sensitivity study, by F. Pacifico, G.A. Folberth, S. Sitch, J.M. Haywood, P. Artaxo, and L.V. Rizzo

The manuscript has been improved substantially, and all the reviewers' points have been addressed in the revised manuscript and/or the rebuttals. Unfortunately, some fairly important information has been relegated to the Supplement, where few readers will see it. In fact, the supplementary text is very brief, and there is no reason why it should not be incorporated into the main text, while the supplementary figures can be kept as a supplement.

Reply: We have kept the supplementary figures in the supplement and moved the supplementary text into the main manuscript.

Specifically I would like the authors to do the following:

1) Move the text "Model evaluation of surface temperature..." to the main text, probably best after the "Description of..." section. Some comments about how well the seasonality of precipitation is captured would also be in order. There is a tendency for models either to capture the distribution of precip, or the seasonal cycle in the Amazon, but not both. The text can then refer to supplemental figures, labeled S1, etc.

Reply: We have moved the supplementary text to page 8 line 217-222. We have also added some text and a figure (Figure S03) on the seasonal cycle of precipitation. This is the text: "HadGEM2 is able to reproduce the main spatial distribution of surface temperature (Figure S1) and precipitation (Figure S2). Surface temperature simulated with HadGEM2 exhibits a bias in the region of up to

27 2°C colder than in the observations over the Amazon forest. Simulated precipitation rate is in
28 reasonable agreement with observations. The model is able to reproduce the main features of the
29 seasonal cycle of precipitation, but tends to simulate less precipitation in September and November
30 than the observations (Figure S03)."
31
32
33 2) *The same applies to the section on Model evaluation of NPP.*
34 *3) As far as I could tell, the Model evaluation of O3 only appears in the supplement. This is*
35 *crucial information and should be prominently visible. The reader should also be told, in the main*
36 *text, that the model performs much more poorly in the tropics than the ACCENT mean (Figure S4).*
37 *One a positive note, the reader should be told that agreement is better in the few tropical*
38 *continental profiles than the marine ones. This might also be a good opportunity to drive home the*
39 *point that we really need more long- term continental ozone measurements at tower sites to remove*
40 *the near-surface bias.*
41
42 Reply: We have moved the following text from the supplementary material to page 8 line 224-243:
43 "Simulated HadGEM2 NPP is compared against a meta-analysis of field data from the Ecosystem
44 Model Data Model Intercomparison project (EMDI) (Olson et al., 2001). Measurements from the 81
45 'class A' ("well documented and intensively studied") sites, representative of all major global
46 biomes, are compared against our simulations. Traditionally, global vegetation models
47 underestimate NPP in tropical ecosystems, and tend towards an asymptote of ~1000 g C m^{-2}
48 (Prentice et al., 2007). HadGEM2 is able to reproduce the main geographical variations of NPP
49 globally (Figure S4), especially in the Northern Hemisphere, where more plentiful observations are
50 available. In addition HadGEM2 is able to simulate higher tropical NPP, although it appears to
51 overestimate NPP over the Amazon region.
52 Ozone concentration simulated with HadGEM2-UKCA-ExtTC agrees better with observations at

higher altitudes and higher latitudes (Figure S5). The model performs more poorly than the ACCENT mean over tropical areas, especially closer to the surface. Comparison with a selection of observed profiles of O_3 concentration shows the model overestimates O_3 for some locations but is in extremely good agreement for others. Over the tropics the agreement is better in the few continental profiles than the marine environment (Figure S6). Some differences may be expected given that the observations are from campaigns with specific meteorological conditions, while the model simulations represent a multi-year mean from the model. Comparison with a selection of surface O_3 observations (Figure S7) confirms again how the model shows a better agreement with observations taken at higher latitudes."

4) The response to my comment on O3 deposition missed the point. I had asked for a comparison of deposition velocities, not deposition fluxes. The former are a characteristic of the model and are concentration independent. The text in the supplement is also very brief and does not give a proper evaluation. It is also not clear, which "Table 1" is referred to. I didn't find a Table. I expect a more detailed response to this issue.

Reply: We have replaced the previous figure on deposition fluxes with Figure S08 on deposition velocities. We have also added some text to comment on this at page 14 lines 431-440: "A comparison with Rummel et al. (2007) indicates that ozone dry deposition velocities on average compare favourably with observations. Rummel at al. (2007) reported day-time velocities of up to 2 cm/s and night-time velocities of typically around 0.5 cm/s during the wet season and velocities between 0.3 cm/s and 1.0 cm/s during day-time and 0.3 cm/s and 0.8 cm/s during the dry season for one site in the Amazon region. HadGEM2-ES predicts annual mean O_3 deposition velocities of 0.5 to 0.6 cm/s (see Figure S8) in fair agreement with the observations. Furthermore, the model is able to capture well the variability between the wet season and the dry season. However, more data are

needed to conduct a robust evaluation, but this admittedly crude comparison is sufficient to demonstrate a basic capability of HadGEM2-ES to reproduce observed ozone deposition velocities in the Amazon region to a reasonable degree."

5) In their response 6 to referee #1, the authors do not address the referee's question about biofuel. They should state the percentage contribution of biofuels to the fire emissions.

At page 9 line 257-259 we have added: " The residential and commercial combustion contribution accounts 1 and 8% of the total annual biomass burning emissions of CO and NO_x respectively."
We do not have the means to separate the contribution of biofuels, as this is one of the components of the residential and commercial combustion contribution it will be less than the percentages stated above.

6) Referee #2, response 2: This response about the use of diurnal cycles is honest, but not very satisfying. I won't ask to rerun the model with an improved mechanism, of course, but just for your information, there are relatively easy ways to accomplish this, for example in: Konovalov, I. B., Berezin, E. V., Ciais, P., Broquet, G., Beekmann, M., Hadji-Lazaro, J., Clerbaux, C., Andreae, M. O., Kaiser, J. W., and Schulze, E.-D., Constraining CO2 emissions from open biomass burning by satellite observations of co- emitted species: a method and its application to wildfires in Siberia: Atmos. Chem. Phys., 14, 10,383–10,410, doi:10.5194/acp-14-10383-2014, 2014. Using a diurnal cycle and a better intra-monthly variation is likely to result in significant improvements. At least it did in our study.

We thank the Editor for this advice.

7) The quality of the figures in the pdf I received is still poor, with fuzzy text and graphs. This may just be the effect of Copernicus compressing excessively. Make sure that the final graphs are clean and crisp.

We made sure the quality of the figures is good.

Biomass burning related ozone damage on vegetation over the Amazon forest: A model sensitivity study.

F. Pacifico[1], G. A. Folberth[2], S. Sitch[3], J. M. Haywood[1,2], L. V. Rizzo[5], F. F. Malavelle, and P. Artaxo[4]

[1] College of Engineering, Mathematics and Physical Sciences, University of Exeter, Exeter, UK

[2] Met Office Hadley Centre, Exeter, UK

[3] Geography, College of Life and Environmental Sciences, University of Exeter, Exeter, UK

[4] Department of Applied Physics, Institute of Physics, University of Sao Paulo, Sao Paulo, Brazil

[5] Department of Earth and Exact Sciences, Institute of Environmental, Chemical and Pharmaceutics Sciences, Federal University of Sao Paulo, Sao Paulo, Brazil

Abstract

The HadGEM2 Earth System climate model was used to assess the impact of biomass burning on surface ozone concentrations over the Amazon forest and its impact on vegetation, under present-day climate conditions. Here we consider biomass burning emissions from wildfires, deforestation fires, agricultural forest burning, residential and commercial combustion. Simulated surface ozone concentration is evaluated against observations taken at two sites in the Brazilian Amazon forest for years 2010 to 2012. The model is able to reproduce the observed diurnal cycle of surface ozone mixing ratio at the two sites, but overestimates the magnitude of the monthly averaged hourly measurements by 5-15 ppb for each available month at one of the sites. We vary biomass burning

emissions over South America by +/-20, 40, 60, 80 and 100% to quantify the modelled impact of biomass burning on surface ozone concentrations and ozone damage on vegetation productivity over the Amazon forest. We used the ozone damage scheme in the "high" sensitivity mode to give an upper limit for this effect. Decreasing South American biomass burning emissions by 100% (i.e. to zero) reduces surface ozone concentrations (by about 15ppb during the biomass burning season) and suggests a 15% increase in monthly mean net primary productivity averaged over the Amazon forest, with local increases up to 60%. The simulated impact of ozone damage from present-day biomass burning on vegetation productivity is about 230 TgC/yr. Taking into account that uncertainty in these estimates is substantial, this ozone damage impact over the Amazon forest is of the same order of magnitude as the release of carbon dioxide due to fire in South America; in effect to potentially double the impact of biomass burning on the carbon cycle.

148

149 **Introduction**

150

151 Biomass burning is a global source of aerosol and trace gases, including ozone (O_3) precursors, and
152 can lead to local and regional O_3 pollution. Tropospheric O_3 is a greenhouse gas and, above
153 background concentrations, an air pollutant: it is harmful to human health (e.g. Lippmann 1993;
154 Burnett et al., 1997) and it damages plants (e.g. Rich et al., 1964; Fiscus et al., 2005; Felzer et al.,
155 2007; Ainsworth et al., 2012). Tropospheric O_3 is a product of photochemical reactions whose main
156 precursors are nitrogen oxides (NO_x), carbon monoxide (CO), methane (CH_4) and volatile organic
157 compounds (VOCs) (Seinfeld and Pandis, 1998). VOCs are particularly important in Amazonia
158 because of the large natural biogenic and biomass burning emissions (Karl et al., 2007).

159

160 In the Amazon forest, biomass burning is mostly anthropogenic, and mainly occurs during the dry
161 season (August to October). Biomass burning emissions drastically change the composition of the
162 atmosphere, e.g. diurnal maximum mixing ratios of tropospheric O_3 varies from 12 parts per billion
163 (ppb), during the wet season, to values as high as 100 ppb in the biomass burning affected dry
164 season (Kirkman et al., 2002, Sigler et al., 2002, Artaxo et al., 2002, 2005, Rummel et al., 2007).

165

166 Surface O_3 mixing ratios over 40 ppb are known to produce visible leaf injury and damage to plants,
167 reducing crop productivity and posing a threat to food security; nonetheless different climatic
168 conditions (e.g. soil moisture and water stress) also play a role in determining leaf stomatal closure
169 and hence there will be variable impacts of the same O_3 concentrations (Ashmore, 2005), e.g.
170 tropical rainforest vegetation may be particularly sensitive to surface O_3, even at concentrations
171 below 40ppb (a threshold associated with extra-tropical vegetation), due to high stomatal
172 conductances. Moreover, tropical vegetation evolved in low background O_3 concentrations and
173 could be more sensitive to O_3. In leaves, cellular damage caused by O_3 not only reduces

174 photosynthetic rates but also requires increased resource allocation to detoxify and repair leaves
175 (Ainsworth et al., 2012). Ozone damage to vegetation reduces plant productivity, decreasing the
176 amount of carbon absorbed by plants, hence has an impact on climate via and indirect radiative
177 forcing (Sitch et al., 2007).
178
179 Tropical rain forests play an important role in the global carbon budget, as they cover 12% of the
180 Earth's land surface and contain around 40% of the terrestrial biosphere's carbon (Ometto et al.,
181 2005, Taylor & Lloyd, 1992). It has been estimated that they may account for as much as 50% of
182 the global net primary productivity (Grace et al., 2001). Depending on age, land use and large scale
183 meteorological conditions, tropical forest ecosystems can act as net carbon sources, sinks, or they
184 can be in approximate balance (Lloyd. et al., 2007, Gatti et al., 2013), but it is uncertain if global
185 environmental changes are forcing these ecosystems outside their range of natural variation (Sierra
186 et al., 2007). However, biomass burning may further reduce natural sinks in the neighbouring intact
187 forest, via air pollution and O_3 damage on vegetation, and thus current estimates of the effects of
188 biomass burning on the carbon cycle (Le Quéré et al., 2009) may be underestimated. Biomass
189 burning is also an important aerosol source: regional levels of particulate matter are very high in the
190 dry season in Amazonia (Artaxo et al., 2013), and the increase in diffuse radiation due to changes in
191 aerosol loadings can increase net ecosystem exchange (NEE) quite significantly (Oliveira et al.,
192 2007, Cirino et al., 2013). After a certain level of aerosol optical depth, the decrease in radiation
193 fluxes can reduce significantly NEE over Amazonia (Cirino et al., 2013). This study does not
194 consider the effects of the changes in diffuse radiation due to biomass burning on photosynthesis, or
195 the impact of aerosols on O_3 chemistry via changing photolysis rate. That will be the focus of a
196 separate study. Our specific aim is to estimate the effect of O_3-induced changes on vegetation
197 productivity due to biomass burning.
198
199 Importantly, Sitch et al. (2007) performed their assessment of the potential impact of O_3 on

vegetation using an offline simulation where monthly mean O_3 concentrations derived with a global chemistry climate model were used in determining the impacts of O_3 damage. Here we use an online flux-gradient approach to quantify the impact of biomass burning on surface O_3 concentration and O_3 damage on vegetation over the Amazon forest (see model description). The HadGEM2 (Hadley Centre Global Environment Model 2; Collins et al., 2011; Martin et al., 2011) Earth System climate model is used to study these interactions. We show results of the evaluation of surface O_3 simulated with HadGEM2 against observations in the Amazon forest and model experiments quantifying the impact of biomass burning on plant productivity.

Methods

We used HadGEM2 to simulate surface O_3 concentrations and O_3 damage on vegetation for present-day (2001-2009) climate conditions. Our version of HadGEM2 includes the O_3 damage scheme developed by Sitch et al. (2007). We evaluated simulated surface O_3 against observations taken at two sites in the Amazon forest: Porto Velho (Brazil; 8.69∞S; 63.87∞W), a site heavily impacted by biomass burning emissions, and site ZF2 in the Cuieiras forest reserve in Central Amazonia (Brazil; 2.59∞S; 60.21∞W). A description of the sites can be found in Artaxo et al. (2013). In a sensitivity study we varied biomass burning emissions over South America by +/-20, 40, 60, 80, 100% to quantify the potential impact of biomass burning on surface O_3 concentrations and O_3 damage over the Amazon forest.

Model description

HadGEM2 is a fully coupled Earth-system model (Collins et al., 2011). It is built around the

HadGEM2 atmosphere-ocean general circulation model and includes a number of earth system components: the ocean biosphere model diat-HadOCC (Diatom-Hadley Centre Ocean Carbon Cycle, a development of the HadOCC model of Palmer and Totterdell, 2001), the Top-down Representation of Interactive Foliage and Flora Including Dynamics (TRIFFID) dynamic global vegetation model (Cox, 2001), the land-surface and carbon cycle model MOSES2 (Met Office Surface Exchange Scheme; Cox et al. 1998, 1999; Essery et al. 2003), the interactive Biogenic Volatile Organic Compounds (iBVOC) emission model (Pacifico et al., 2012), the United Kingdom Chemistry and Aerosol (UKCA) model (O'Connor et al., 2014) and an interactive scheme of O_3 damage on vegetation (Sitch et al., 2007; Clark et al., 2011).

The configuration used here is a version of HadGEM2-UKCA with extended tropospheric chemistry (N96L38), the resolution is 1.25° latitude x 1.875° longitude (~200 x 140 km) at the equator with 38 vertical levels extending up to 39 km altitude. The land-based anthropogenic, biomass burning, and shipping emissions are taken from Lamarque et al. (2010), and represent a decadal (1997-2006) mean centered on the year 2000. The use of an emission pattern from 1997-2006 can lead to an overestimation of O_3 concentrations by the model, since the emissions vary on a year to year basis and are expected to be lower in recent years due to the reduction in Amazonian deforestation via burning, consequently reducing the amount of O_3 precursors. HadGEM2 runs at a 30-minute time step with the exception of global radiation, which is updated every 3 hours and provides radiative fluxes between those time steps via interpolation. This configuration is described and evaluated in O'Connor et al. (2014) with the exception of the Extended Tropospheric Chemistry (ExtTC) that has been applied in this work. The ExtTC mechanism has been designed to represent the key species and reactions in the troposphere in as much detail as is necessary to simulate atmospheric composition-climate couplings and feedbacks while retaining the capability to conduct decade-long climate simulations. UKCA-ExtTC simulates the spatial distribution and evolution in time of 89 chemical species, 63 of which are model tracers. The model includes

252 emissions from anthropogenic, biogenic, soil, and wildfire sources for 17 species: nitrogen oxides
253 (NO_x = NO +NO_2), CH_4, carbon monoxide (CO), hydrogen (H_2), methanol, formaldehyde,
254 acetaldehyde and higher aldehydes, acetone, methyl ethyl ketone, ethane (C_2H_6), propane (C_3H_8),
255 butanes and higher alkanes, ethene (C_2H_4), propene (C_3H_6), isoprene, (mono)terpenes, and a lumped
256 species representing aromatics (toluene + xylene) from anthropogenic sources.
257
258 Emissions of biogenic species (isoprene, terpenes, methanol, acetone) are computed by iBVOC and
259 provided to UKCA at every time step. The isoprene emission scheme is that of Pacifico et al.
260 (2011). Terpenes, methanol, and acetone emissions are simulated with the model described in
261 Guenther et al. (1995). Anthropogenic and wildfire emissions are prescribed from monthly mean
262 emission data sets prepared for CMIP5 using the historic scenario (Lamarque et al., 2010). Given
263 the difficulty in prescribing a diurnal cycle for fire emissions, these monthly mean emissions are
264 kept constant during the day. Wetland methane emissions are prescribed from data from Gedney et
265 al. (2004). Soil-biogenic NO_x emissions are prescribed using the monthly distributions provided by
266 the Global Emissions Inventory Activity (http://www.geiacenter.org/inventories/present.html),
267 which are based on the global empirical model of soil-biogenic NO_x emissions of Yienger and Levy
268 (1995). NO_x emissions from global lightning activity are parameterized based on the convective
269 cloud top height following Price and Rind (1992, 1994) and are thus sensitive to the model climate.
270 UKCA also includes a dry deposition scheme based on the resistance in-series approach as outlined
271 in Wesely (1989). Physical removal of soluble species is parameterized as a first-order loss process
272 based on convective and stratiform rainfall rates (Collins et al., 2011).
273
274 The TRIFFID vegetation module of HadGEM2 simulates the dynamics of five plant functional
275 types (PFTs): broadleaf trees, needleleaf trees, shrubs, and C_3 and C_4 grass (i.e., grasses using the
276 C_3 and C_4 photosynthetic pathway, respectively). Changes in the extent of croplands over time are
277 not simulated but are prescribed from land use maps prepared for the Coupled Model

Intercomparison Project 5 (CMIP5, Taylor et al., 2012). Here we use the historic (1850–2000; Hurtt et al., 2009) data sets, as described in Jones et al. (2011). A further four surface types (urban, inland water, bare soil, and ice) are used in the land-surface scheme for the calculation of water and energy exchanges between the land and the atmosphere. Each model grid box can include varying proportions of several vegetation and/or surface types. The model does not include interactive deforestation due to fire.

The parameterization of O_3 damage on vegetation is that of Sitch et al., (2007). This scheme uses a flux-gradient approach to model O_3 damage, rather than empirical approaches based on the accumulated O_3 exposure above 40 ppb (e.g. Felzer, et al. 2005). The Sitch et al. (2007) parameterization assumes a suppression of net leaf photosynthesis by O_3 that varies proportionally to the O_3 flux through stomata above a specified critical O_3 deposition flux. The critical deposition flux depends on O_3 concentration near the leaves, but also on stomatal conductance. This scheme also includes a relationship between stomatal conductance and photosynthesis, determining a reduction in stomatal conductance through O_3 deposition. As the O_3 flux itself depends on the stomatal conductance, which in turn depends upon the net rate of photosynthesis, the model requires a consistent solution for the net photosynthesis, stomatal conductance and the O_3 deposition flux. This approach to modelling O_3 effects on photosynthesis accounts for the complex interaction between CO_2 and O_3 effects, and can be used to study future climate impacts. This scheme includes a 'high' and 'low' parameterization for each PFT to represent species more sensitive and less sensitive to O_3 effects; in our analysis we use the 'high' sensitivity mode to establish the maximum response. The model was calibrated with data from temperate and boreal vegetation. Calibration data for other ecosystems, including tropical vegetation, are currently unavailable.

Description of the model experiments

304 All simulations use HadGEM2 in its atmosphere-only configuration, i.e., with all implemented
305 couplings between atmosphere and land surface (including carbon cycle) active but without the
306 atmosphere-ocean coupling. HadGEM2 was initialized with equilibrium concentrations of the major
307 chemical components (O_3, CO, H_2, total reactive nitrogen (NO_y), BVOCs) taken from the CMIP5
308 simulation (see description of the simulations in Jones et al., 2011). Methane mixing ratios were
309 prescribed as specified by CMIP5, with values of 1750 ppb for present-day. The decade-mean CO2
310 atmospheric mixing ratio was 368 ppm.
311 Monthly means of sea surface temperature and sea ice cover were prescribed using climatologies
312 derived from the appropriate decade of the Hadley Centre CMIP5 transient climate run Jones et al.,
313 (2011). The vegetation distribution for each of our simulations was prescribed using the simulated
314 vegetation averaged for the same decade from this transient climate run, on which we superimposed
315 crop area as given in the CMIP5 historic and future land use maps (Hurtt et al., 2009; Riahi et al.,
316 2007).
317
318 We performed a 9-year (2001-2009) control simulation for present-day climate conditions
319 initialized from a centennial transient climate simulation with ocean couplings (Jones et al., 2011).
320 We analysed the last 8 years of the simulation, as the first year of simulation was used as spin-up. A
321 single year is considered sufficient for spin-up because one year is around five times longer than the
322 lifetime of the longest lived atmospheric species (with the exclusion of methane) involved in O_3
323 chemistry. The control simulation was driven by anthropogenic and wildfire emissions of trace
324 gases and aerosols via historical scenarios (Global Fire Emissions Database GFEDv2; Lamarque et
325 al., 2010; Van der Werf et al., 2006) of anthropogenic and wildfire emissions.
326
327 HadGEM2 is able to reproduce the main spatial distribution of surface temperature (Figure S1) and
328 precipitation (Figure S2). Surface temperature simulated with HadGEM2 exhibits a bias in the
329 region of up to 2∞C colder than in the observations over the Amazon forest. Simulated precipitation

rate is in reasonable agreement with observations. The model is able to reproduce the main features of the seasonal cycle of precipitation, but tends to simulate less precipitation in September and November than the observations (Figure S03).

Simulated HadGEM2 NPP is compared against a meta-analysis of field data from the Ecosystem Model Data Model Intercomparison project (EMDI) (Olson et al., 2001). Measurements from the 81 'class A' ("well documented and intensively studied") sites, representative of all major global biomes, are compared against our simulations. Traditionally, global vegetation models underestimate NPP in tropical ecosystems, and tend towards an asymptote of ~1000 g C m^{-2} (Prentice et al., 2007). HadGEM2 is able to reproduce the main geographical variations of NPP globally (Figure S4), especially in the Northern Hemisphere, where more plentiful observations are available. In addition HadGEM2 is able to better simulate higher tropical NPP.

Ozone concentration simulated with HadGEM2-UKCA-ExtTC agrees better with observations at higher altitudes and higher latitudes (Figure S5). The model performs more poorly than the ACCENT mean over tropical areas, especially closer to the surface. Comparison with a selection of observed profiles of O_3 concentration shows the model overestimates O_3 for some locations but is in extremely good agreement for others. Over the tropics the agreement is better in the few continental profiles than the marine environment (Figure S6). Some differences may be expected given that the observations are from campaigns with specific meteorological conditions, while the model simulations represent a multi-year mean from the model. Comparison with a selection of surface O_3 observations (Figure S7) confirms again how the model shows a better agreement with observations taken at higher latitudes.

We also perform 10 experiments that differ from the control simulation in terms of assumed biomass burning emissions, i.e. biomass burning emissions over South America are either increased

356 or decreased by +/-20, 40, 60, 80, 100%, while emissions over the rest of the world are kept
357 unchanged. The vegetation distribution was not adjusted for loss of vegetation due to fire. We
358 define biomass burning emissions as those from wildfires, deforestation fires, agricultural forest
359 burning, residential and commercial combustion, including fuel wood burning, charcoal production
360 and biofuel combustion for cooking and heating (Lamarque et al., 2010). The dominant fire types in
361 South America are from deforestation and degradation fires in an arc around Amazonia, with some
362 regional hotspots of agricultural burning (see Figure 13 in Van der Werf et al., 2010). Between
363 2001 and 2009 the percentage contribution to annual fire emissions from fire types (deforestation
364 and degradation, grassland and savanna, woodland, forest, agriculture) are (59%, 22%, 10%, 8%,
365 2%) over Southern Hemisphere South America (Figure 13 van der Werf et al., 2010), with minor
366 differences in this region between this dataset (Global Fire Emissions Database GFEFv3) and the
367 earlier GFEDv2 used in this study (see Fig. 16 in Van der Werf et al., 2010). The residential and
368 commercial combustion contribution accounts for 1 and 8% of the total annual biomass burning
369 emissions of CO and NO_x respectively.
370
371 This set of experiments allows us to simulate the impact of biomass burning on surface O_3 and
372 vegetation productivity. The control simulation was also used to evaluate surface O_3 mixing ratios
373 against measurements over the Amazon forest.
374
375
376 **Model site-level Evaluation**
377
378 Over the data-sparse Amazonian region, comprehensive spatial data sets of surface O_3
379 concentration are extremely limited. We evaluated simulated surface O_3 against observations from
380 two sites that have full annual analyses of O_3 concentration: Porto Velho (Brazil; 8.69∞S;
381 63.87∞W) and site ZF2 in the Cuieiras forest reserve (Brazil; 2.59∞S; 60.21∞W). O_3 mixing ratios

were measured with a UV absorption analyser (Thermo 49i, USA). Observations from both sites have an estimated 4% uncertainty, considering zero noise, zero and span drifts reported in the instrument manual, and the frequency of zero and span checks performed along the experiments.

The Porto Velho sampling site is located in a forest reserve about 5 km NE (generally upwind) from the city of Porto Velho. Large land use change and regional biomass burning makes its atmospheric conditions characteristic of those of the Amazon forest with significant human interference (Brito et al., 2014). The whole region of Porto Velho has been subject to land use change since the 1980s. In Porto Velho, the dry season is from June to October and the wet season from November to May. Measurements of surface O_3 mixing ratios were taken from November 2011 to October 2012 in a forest clearance, at 5 m a.g.l..

The Cuieiras forest reserve in Central Amazonia encloses 380 km^2 of pristine tropical rainforest forest. The reserve is located in the central Amazon Basin, 60 km NNW of downtown Manaus and 40 km from the metropolis margins. This site is relatively undisturbed, as no biomass burning occurs in the forest reserve. Here rain showers are frequent with a short dry season from July to October. Measurements were taken at 39 m a.g.l. at the TT34 tower. The forest canopy height near the tower varied between 30 and 35 m, and the site is described in Martin et al. (2010), Rizzo et al. (2013) and Artaxo et al. (2013). Most of the time, the prevailing trade winds blow over 2000 km of the intact tropical forest before reaching the measurement tower. However, the site was also affected by regional transport of pollutants, either from biomass burning or urban sources (Rizzo et al., 2013). Measurements of surface O_3 mixing ratios were taken from April 2010 to June 2012, with the exclusion of a few months due to instrument maintenance.

We compared simulated (averaged over 8 years of simulations) against observed average O_3 diurnal cycles at each site for each available month. The model overestimates observed monthly averaged

hourly O_3 mixing ratios at the surface by about 5-15 ppb for all months at the Porto Velho site, but it reproduces the diurnal and seasonal cycle, including those months affected by biomass burning, i.e. August and September, at the Porto Velho site (Figure 1). The model is able to reproduce the diurnal cycle, including magnitude, at the ZF2 site for about 8 months out of 24. The model overestimates surface monthly averaged hourly O_3 mixing ratios by about 5-10 ppb for the rest of months, which are also the months with lower surface O_3 mixing ratios (Figure 2).

Results

Our analysis is focused on the region enclosed in the red rectangle in figure 3, this is a highly vegetated region with homogeneous topography, and it includes the two sites used for the model evaluation (Porto Velho and ZF2 in the Cuieiras forest reserve). This region of analysis is covered by two PFTs in HadGEM2: broadleaf trees, which is the predominant, and C_3 grass (Figure 3).

Surface O_3 mixing ratios simulated with HadGEM2 are higher during the months of August, September and October over the Amazon forest, and in particular over our region of analysis, because of the higher biomass burning emissions in the model during these months. Monthly average surface O_3 mixing ratios in our control simulation peaks at 55-60 ppb in this region (Figure 4), while the average over the region of analysis is peaked at about 30 ppb in August and September, less in October (Figure 5a, black line).

Monthly total Net Primary Productivity (NPP) in our control simulation reaches its minimum during the months of August and September (Figure 5b, black line), at about 300 TgC/month, corresponding to the end of the dry season.

434 Decreasing biomass burning emissions over South America by -20%, -40%, -60%, -80%, -100%
435 decreases surface O_3 mixing ratios and increases net productivity. Vice versa, increasing biomass
436 burning emissions over South America by +20%, +40%, +60%, +80%, +100% increases surface O_3
437 mixing ratios over the region of analysis and subsequently reduces net productivity because of O_3
438 damage on vegetation (Figure 5c).
439 These sensitivity tests suggest that decreasing biomass burning emission by 100% over South
440 America brings monthly mean surface O_3 mixing ratios averaged over the region of analysis to
441 about the observed 15 ppb for each month (Figure 5a, dark blue line), even during the dry season,
442 with no values over 35 ppb for any grid-cell (Figure 6). Increasing biomass burning emissions by
443 100% suggests that monthly mean mixing ratios of surface O_3 averaged over the region of analysis
444 reach 40 ppb in August (Figure 5a), with peaks of about 65-70 ppb in some grid-cells (Figure 6a).
445 For both increases and decreases of between 20 and 80% in South American biomass burning the
446 model simulates almost linear changes in surface O_3 mixing ratios (Figure 6, the figure shows
447 increases and reductions by 40, 60 and 100%).
448
449 Suppressing biomass burning emissions (i.e. decreasing biomass burning emission by 100%) over
450 South America increases total NPP over the region of analysis by about 15%, to about 350-370
451 TgC/month, with peak increases of 60% for a few grid-cells, in August and September (Figure 6b):
452 this quantifies the impact of present-day biomass burning on vegetation productivity. When
453 increasing biomass burning emissions over South America by 100%, monthly total NPP over the
454 region of analysis is reduced by about 10%, i.e. to about 250 TgC/month, in August and September
455 (Figure 5b), with peak values of 50-60% reductions for few grid-cells (Figure 6c). For reductions by
456 20 to 80% in South American biomass burning the model varies NPP almost linearly (Figure 5c).
457 However, the increase in South American biomass burning by 20 to 80% determine a very similar
458 decrease in NPP, e.g. between 7 and 10% decrease in August (Figure 5c). Both increasing and
459 reducing South American biomass burning from 20 to 80% increases the number of grid-cells

460 where a significant variation of NPP takes place (Figure 6b). The percentages given above are
461 significant against inter-annual variability in the control simulation, i.e. we only take into account of
462 the variations above one standard deviation in the control simulation. We also exclude from our
463 analysis the grid-cells with low productivity, i.e. where NPP in the control simulation is below 50
464 gC/m^2/month (i.e. we focus on high productivity regions, e.g. forests).
465
466
467 **Discussion and Conclusions**
468
469 The HadGEM2 model overestimates the magnitude of the O_3 diurnal cycle at the two sites used in
470 the evaluation. Overestimation of simulated O_3 in the Amazonian boundary layer has been observed
471 in other modelling studies, especially in clean air conditions (Bela et al., 2014). Nonetheless, our
472 model reproduces the main features of the diurnal and seasonal cycle. In particular, the model is
473 able to reproduce the increase in surface O_3 during the biomass burning season.
474
475 As stated earlier in the model description section, biomass burning emissions are prescribed as
476 monthly mean and kept constant during the day, and this can have an impact on the hourly and day-
477 to-day variation of surface O_3. For example, O_3 production will respond differently if biomass
478 burning emissions occur during the day or at night, affecting simulated surface O_3 mixing ratios.
479 These issues can be improved by modelling fire and biomass burning emissions interactively. The
480 inclusion of an interactive fire model in HadGEM is currently under development.
481
482 The model overestimates surface O_3 mixing ratios by 5-15 ppb for several months at the ZF2 site in
483 the Cuieiras forest reserve and for all available months at the Porto Velho site. The reasons for these
484 systematic biases in surface O_3 mixing ratio are likely manifold. In a complex, highly coupled

485 system such as the HadGEM2 Earth System Model (ESM) it is not always easy to disentangle all
486 processes and attribute model biases to specific components.
487 We attribute the systematic biases in the surface O_3 mixing ratio to the following, most likely
488 reasons:
489 1. Model resolution in both the horizontal and the vertical dimension
490 2. Uncertainties in emissions, both magnitude, seasonality and location
491 3. Uncertainties in the O_3 dry deposition at the surface
492 Other factors such as uncertainties in the chemical mechanism, the photolysis rates, lightning NO_x
493 production over the area and transport of O_3 and precursors will certainly contribute. We will
494 briefly discuss the three most important (in our opinion) factors that contribute to the systematic
495 biases.
496
497 The relatively coarse resolution of a global ESM simulates mixing ratios of trace species (both trace
498 gases and aerosols) that represent averages over large areas. This issue has been discussed
499 previously in the literature, mostly in relation to air quality modelling (see, e.g., Valari and Menut,
500 2008; Tie et al., 2010; Appel et al. 2011; Thompson and Selin, 2012). In our case one grid box
501 equals approximately 30,000 km^2 (i.e., 200x150 km^2 in longitude and latitude). The implicit
502 averaging pertains both to emission and concentration fields; the predominant consequence is a
503 dilution in each grid-cell. Depending on the chemical regime, this can lead to reduced or enhanced
504 net O_3 production. Additionally, HadGEM2-ES has a relatively coarse vertical resolution.
505 HadGEM2-ES has a lowest model layer depth of 40m (global average) and the vertical profile of O_3
506 will undoubtedly show a gradient as the loss mechanism for O_3 is dominated by the surface (e.g.
507 Colbeck and Harrison, 1967). The measurement level may explain part of the model overestimation,
508 since it is well known that O_3 mixing ratios strongly decrease with height due to deposition within
509 the canopy. The lowest layer of the model has a midpoint height 20 metres above the displacement
510 height for the particular gridbox (generally approximated as 2/3 of the average height of the

511 obstacle, in this case the canopy), while measurements were taken at 5 m and 39 m a.g.l.,
512 respectively, at Porto Velho and ZF2 which are located either in or just above canopy level.
513 Rummel et al. (2007) reports a 5-15 ppb O_3 decrease from 52 to 11 m a.g.l. in a forest site in
514 Amazonia. This steep gradient near the surface is due to surface deposition but also due to in-
515 canopy chemical processing (c.f., e.g., Stroud et al., 2005; Gordon et al., 2014). The latter is not
516 represented in HadGEM2-ES.
517
518 The remote environment of the Amazon forest is dominated by relatively high concentrations of
519 VOC, particularly of biogenic origin, and low concentrations of nitrogen oxides, NO_x. It is a NO_x-
520 limited environment. In such an environment O_3 is destroyed by reactions with BVOC (mainly
521 isoprene and (mono-)terpenes). This destruction is more pronounced the higher the BVOC
522 concentration becomes. Consequently, conditions in the global model are likely to differ from that
523 of a measurement at a specific point such as those we compare to in Figures 1 and 2. It is a known
524 problem in model evaluation.
525
526 Another issue related to model resolution, when comparing global models to point-like
527 observations, is the uncertainty in global emission inventories, both with respect to magnitude and
528 location. In particular the latter will result in discrepancies between modelled concentrations of O_3
529 and its precursors and point-like observations. But the uncertainties in emission magnitude are also
530 substantial and can reach a factor of two or more in case of biogenic VOC (e.g., Guenther et al.,
531 2006; Arneth et al., 2008, 2011; Pacifico et al., 2011, 2012).
532
533 Thirdly, and again related to model resolution, is the representation of O_3 dry deposition at the
534 surface. Its magnitude and diurnal cycle will depend on boundary layer turbulence, surface
535 roughness, land surface type, vegetation type, soil moisture, photosynthetic activity, and more. In a
536 recent sensitivity study by Folberth et. al (in preparation) O_3 surface concentrations showed the

largest sensitivity to perturbations in O_3 surface dry deposition fluxes. Underestimating O_3 surface dry deposition, in particular during the night preventing a complete flush of the PBL with respect to O_3, will lead to systematic biases.

A comparison with Rummel et al. (2007) indicates that ozone dry deposition velocities on average compare favourably with observations. Rummel at al. (2007) reported day-time velocities of up to 2 cm/s and night-time velocities of typically around 0.5 cm/s during the wet season and velocities between 0.3 cm/s and 1.0 cm/s during day-time and 0.3 cm/s and 0.8 cm/s during the dry season for one site in the Amazon region. HadGEM2-ES predicts annual mean O_3 deposition velocities of 0.5 to 0.6 cm/s (see Figure S8) in fair agreement with the observations. Furthermore, the model is able to capture well the variability between the wet season and the dry season. However, more data are needed to conduct a robust evaluation, but, this admittedly crude comparison is sufficient to demonstrate a basic capability of HadGEM2-ES to reproduce observed ozone deposition velocities in the Amazon region to a reasonable degree.

Interestingly, however, the latter process may also represent a redeeming feature of the model. According to our model of O_3 plant damage it is the total O_3 flux into the plant that determines the amount of damage caused to the photosynthetic activity and, hence, carbon assimilation. However, the total O_3 flux (or dose) is a function of both O_3 surface concentrations and dry deposition, i.e. for plants there is a compensation effect when concentrations are overestimated while deposition velocities are underestimated. Underestimating the O_3 dry deposition flux implies reduced O_3 plant uptake, and consequently an underestimation of the plant damage and productivity losses. However, it also leads to higher O_3 concentrations, which subsequently act to increase plant O_3 uptake and damage, compensating for the initial effects on productivity. Still, a detailed assessment and quantification of this interdependence of O_3 concentration and dry deposition fluxes is beyond the scope of this study and must be referred to future research.

August, September and October are the months when biomass burning and surface O_3 concentrations are higher over the Amazon forest, but also the months when plant productivity is at its lowest which will tend to suppress the impact of O_3 damage on plant productivity. This is because stomatal conductance is reduced due to water limitations (also accounted for in the model) during the dry season, thus reducing the flux of both carbon dioxide and O_3 into the leaves, and consequently reducing O_3 plant damage.

Ashmore (2005) noted how O_3 exposure is poorly correlated with flux into leaves and also the potential for damagingly high O_3 fluxes in leaves at concentrations significantly below 40 ppb at maximum stomatal conductance. Consequently, global vegetation models as used in this study have adopted flux-based parameterizations to represent O_3 impacts on vegetation, moving away from application of the earlier exposure based metrics, e.g. accumulated O_3 exposure above a threshold of 40 ppb, AOT40.

The parameterization of O_3 damage used in this study is calibrated for high-latitude vegetation. Unfortunately data for calibrating this O_3 damage scheme for tropical vegetation are currently not available and observations of O_3 damage in the Amazon forest are very limited. Observations of O_3 damage on tropical forests are urgently needed, including observations at moderate (e.g. 20-30 ppb) and high surface O_3 mixing ratios.

The simulated impact of present-day biomass burning on vegetation productivity over our area of analysis is about 230 TgC/yr (i.e. the difference between the dark blue line and the black line in Fig. 5b) using the "high" sensitivity mode in the O_3 damage scheme. Taking into account that the uncertainty in these estimates is substantial, this O_3 damage impact over the Amazon forest is of the same order of magnitude as the release of CO_2 due to land fire in South America, as quantified in

van der Werf et al., (2010; 293 TgC/yr from table 7 of that paper); in effect to potentially double the impact of biomass burning on the CO_2 fluxes. This highlights the urgent need for more tropical data on plant O_3 damage to better constrain estimates.

Despite overestimating surface O_3 mixing ratios our model simulates only a moderate reduction in NPP associated with elevated O_3 due to biomass burning emissions. Given that our model systematically overestimates O_3 mixing ratio, assuming accurate dry deposition, and that we use our model in the high sensitivity mode, our simulations where we increase biomass burning emissions by 100% suggest a maximum 10% average reduction in monthly plant productivity, and peak reductions of 50-60% reductions in few grid-cells. This is because, despite the increase in biomass burning, monthly average surface O_3 mixing ratios do not exceed a moderate 40 ppb. Moreover, our model does not include deforestation due to fire, which would reduce vegetation cover when increasing biomass burning emissions in our sensitivity experiments, reducing NPP, and BVOC emissions, further. However, local and daily/hourly impact of O_3 damage on plant productivity can be higher.

Estimates of the magnitude of the reduction in plant productivity due to O_3 damage can be improved with additional field studies and improving the representation of tropospheric O_3 in ESMs (sources, chemistry and sinks). Nevertheless, considering these processes in a coupled system can provide an improvement in robustness of conclusions, as e.g. it can treat processes with a specific diurnal cycle, like photosynthesis and surface O_3, interactively on a short time scale (e.g. half an hour in our model).

Acknowledgments

This work was funded by the Natural Environment Research Council (NERC) South AMerican Biomass Burning Analysis (SAMBBA) project grant code NE/J010057/1. The UK Met Office contribution to this project was funded by the DECC under the Hadley Centre Climate Programme contract (GA01101). The Brazilian contribution was funded by Fundacao de Amparo a Pesquisa do Estado de Sao Paulo (FAPESP, projects 08/58100-2 and 12/14437-9). We thank INPA (Instituto Nacional de Pesquisas da Amazonia) for the coordination work of the LBA Experiment. We thank USP technicians for the support on data sampling: Alcides Ribeiro, Ana Lucia Loureiro, Fernando Morais and Fabio Jorge.

622

623 **References**

624

625 Ainsworth, E. A., Yendrek, C. R., Sitch, S., Collins, W. J. and Emberson, L. D.: The Effects of
626 Tropospheric Ozone on Net Primary Productivity and Implications for Climate Change, Annu. Rev.
627 Plant Biol., 63, 637-61, 2012.

628

629 Appel, K. W., Foley, K. M., Bash, J. O., Pinder, R. W., Dennis, R. L., Allen, D. J. and Pickering,
630 K.: A multi-resolution assessment of the Community Multiscale Air Quality (CMAQ) model v4.7
631 wet deposition estimates for 2002-2006, Geosci. Model Dev., 4, 357-371, 2011.

632

633 Arneth, A., Monson, R. K., Schuregers, G., Niinemets, Ü. and Palmer, P. I.: Why are estimates of
634 global terrestrial isoprene emissions so similar (and why is it not so for monoterpenes), Atmos.
635 Chem. Phys., 8, 4605-4620, 2008.

636

637 Arneth, A., Schurgers, G., Lathiere, J., Duhl, T., Beerling, D. J., Hewitt, N., Guenther, A.: Global
638 terrestrial isoprene emission in models: sensitivity to variability in climate and vegetation, Atmos.
639 Chem. Phys., 11, 8037-8052, 2011.

640

641 Artaxo, P., Martins, J. V., Yamasoe, M. A., Procópio, A. S., Pauliquevis, T. M., Andreae, M. O.,
642 Guyon, P., Gatti, L. V., Leal., A. M. C.: Physical and chemical properties of aerosols in the wet and
643 dry season in Rondônia, Amazonia. J. Geophys. Res., 107, D20, 8081-8095, 2002.

644

645 Artaxo, P., Gatti, L V., Leal, A. M. C, Longo, K. M., de Freitas, S. R., Lara, L. L., Pauliquevis, T.
646 M., Procópio, A. S., Rizzo, L. V.: Atmospheric Chemistry in Amazonia: The forest and the biomass
647 burning emissions controlling the composition of the Amazonian atmosphere, Acta Amazonica,

35(2), 185-196, 2005.

Artaxo, P., Rizzo, L. V., Brito, J. F., Barbosa, H. M. J., Arana, A., Sena, E. T., Cirino, G. G., Bastos, W., Martin, S. T., Andreae. M. O.: Atmospheric aerosols in Amazonia and land use change: from natural biogenic to biomass burning conditions. Faraday Discussions, 2013

Ashmore, M. R: Assessing the future global impacts of ozone on vegetation, Plant Cell Environ., 28, 949-964, 2005.

Bela, M. M., Longo, K. M., Freitas, S. R., Moreira, D. S., Beck, V., Wofsy, S. C., Gerbig, C., Wiedemann, K., Andreae, M. O., and Artaxo, P.: Ozone production and transport over the Amazon Basin during the dry-to-wet and wet-to-dry transition seasons, Atmos. Chem. Phys. Discuss., 14, 14005–14070, 2014

Brito, J., Rizzo, L. V., Morgan, W. T., Coe, H., Johnson, B., Haywood, J., Longo, K., Freitas, S., Andreae, M. O. and Artaxo, P.: Ground based aerosol characterization during the South American Biomass Burning Analysis (SAMBBA) field experiment, Atmos. Chem. Phys. Discuss., 14, 12279-12322, 2014.

Burnett, R. T., Brook, J. R., Yung, W. T., Dales, R. E., Krewski, D.: Association between Ozone and Hospitalization for Respiratory Diseases in 16 Canadian Cities, Environ. Res., 72, 1, 24-31, 1997.

Cirino, G.G., Souza, R. F., Adams, D. K. and Artaxo, P.: The effect of atmospheric aerosol particles and clouds on net ecosystem exchange in Amazonia, Atmos. Chem. Phys. Discuss., 13, 28819–28868, 2013.

674

675 Clark, D. B., Mercado, L. M., Sitch, S., Jones, C. D., Gedney, N., Best, M. J., Pryor, M., Rooney,
676 G. G., Essery, R. L. H., Blyth, E., Boucher, O., Harding, R. J., Huntingford, C. and Cox, P. M.: The
677 Joint UK Land Environment Simulator (JULES), model description – Part 2: Carbon fluxes and
678 vegetation dynamics, Geosci. Model Dev., 4, 701-722, 2011.

679

680 Colbeck, I. and Harrison, R. M.: Dry deposition of ozone: some measurements of deposition
681 velocity and of vertical profiles to 100 metres, Atm. Environ., 19, 11, 1807-1818, 1967

682

683 Collins, W. J., Bellouin, N., Doutriaux-Boucher, M., Gedney, N., Halloran, P., Hinton, T., Hughes,
684 J., Jones, C. D., Joshi, M., Liddicoat, S., Martin, G., O'Connor, F., Rae, J., Senior, C., Sitch, S.,
685 Totterdell, I., Wiltshire, A. and Woodward, S.: Development and evaluation of an Earth-system
686 model-HadGEM2, Geosci. Model Dev., 4, 1051–1075, 2011.

687

688 Cox, P. M., Huntingford, C. and Harding, R. J.: A canopy conductance and photosynthesis model
689 for use in a GCM land surface scheme, J. Hydrol., 212–213, 79–94, 1998._

690

691 Cox, P. M., Betts, R. A., Bunton, C. B., Essery, R. L. H., Rowntree, P. R. and Smith, J.: The impact
692 of new land surface physics on the GCM simulation of climate and climate sensitivity, Clim. Dyn.,
693 15, 183–203, 1999.

694

695 Cox, P. M.: Description of the “TRIFFID” Dynamic Global Vegetation Model, Tech. Note 24, 17
696 pp., Met Off. Hadley Cent., Exeter, U. K, 2001.

697

698 Emmons, L., Hauglustaine, D., Muller, J., Carroll, M., Brasseur, G., Brunner, D., Staehelin, J.,
699 Thouret, V., and Marenco, A.: Data composites of airborne observations of tropospheric ozone and
700 its precursors, J. Geophys. Res., 105, 20497–20538, 2000.
701
702 Essery, R. L. H., Best, M. J., Betts, R. A., Cox, P. M. and Taylor, C. M.: Explicit representation of
703 subgrid heterogeneity in a GCM Land Surface Scheme, J. Hydrometeorol., 4, 530–543, 2003.
704
705 Felzer, B., Reilly, J., Melillo, J., Kicklighter, D., Sarofim, M., Wang, C., Prinn, R. and Zhuang, Q.:
706 Future effects of ozone on carbon sequestration and climate change policy using a global
707 biogeochemical model, Clim. Change 73, 345–373, 2005.
708
709 Felzer, B. S., Cronin, T., Reilly, J. M., Melillo, J. M. and Wang, X.: Impacts of ozone on trees and
710 crops, C. R. Geosci., 339, 784–798, 2007.
711
712 Fiscus, E. L., Booker, F. L., Burkey, K. O.: Crop responses to ozone: uptake, modes of action,
713 carbon assimilation and partitioning, Plant Cell Environ, 28, 997-1011, 2005.
714
715 Fishman et al., 1996 Fishman, J., Hoell, J., Bendura, R., McNeil, R., and Kirchhoff, V.: NASA
716 GTE TRACE A experiment (September October 1992): Overview, J. Geophys. Res., 101,
717 23865–23879, doi:10.1029/96JD00123, 1996.
718
719 Folberth, G. A., Abraham, N. L., Dalvi, M., Johnson, C. E., Morgenstern, O., O'Connor, F. M.,
720 Pacifico, F., Young, P. A., Collins, W. J., and Pyle, J. A.: Evaluation of the new UKCA climate-
721 composition model. Part IV. Extension to Tropospheric Chemistry and Biogeochemical Coupling
722 between Atmosphere and Biosphere, Geosci. Model Dev. (in preparation)
723

724 Gatti et al.: Drought sensitivity of Amazonian carbon balance revealed by atmospheric
725 measurements, Nature 506, 76-80, 2014.
726
727 Gedney, N., Cox, P. M. and Huntingford, C.: Climate feedback from wetland methane emissions,
728 Geophys. Res. Lett., 31, L20503, 2004.
729
730 Gordon, M., Vlasenko, A., Staebler, R. M., Stroud, C., Makar, P. A., Liggio, J., Li, S.-M., and
731 Brown, S.: Uptake and emission of VOCs near ground level below a mixed forest at Borden,
732 Ontario, Atmos. Chem. Phys., 14, 9087–9097, 2014.
733
734 Grace, J., Mahli, Y., Higuchi, N., Meir, P.,: Productivity and carbon fluxes of tropical rain forest.
735 In: J.Roy, H.A.M. (Ed). Global Terrestrial Productivity. Academic Press, San Diego, 2001.
736
737 Guenther, A., Hewitt, C. N., Erickson, D., Fall, R., Geron, C., Graedel, T., Harley, P., Klinger, L.,
738 Lerdau, M., Mckay, W. A., Pierce, T., Scholes, B., Steinbrecher, R., Tallamraju, R., Taylor, J., and
739 Zimmerman, P.: A global model of natural volatile organic compound emissions, J. Geophys. Res.,
740 100(D5), 8873– 8892, 1995.
741
742 Guenther, A., Karl, T., Harley, P., Wiedinmyer, C., Palmer, P. I. and Geron, C.: Estimates of global
743 terrestrial isoprene emissions using MEGAN (Model of Emissions of Gases and Aerosols from
744 Nature), Atmos. Chem. Phys., 6, 3181-321-, 2006.
745
746 Harris, I., Jones, P. D., Osborn, T. J., Lister, D. H.: Updated high-resolution grids of monthly
747 climatic observations – the CRU TS3.10 Dataset, Int. J. Climatol., 34, 632-642, 2014.
748
749 Hurtt, G. C., et al.: Harmonization of global land-use scenarios for the period 1500–2100 for IPCC-

AR5, iLEAPS Newsl., 7, 6–8, 2009.

Jones, C. D., et al.: The HadGEM2-ES implementation of CMIP5 centennial simulations, Geosci. Model Dev. Discuss., 4(1), 689–763, 2011.

Karl, T., Yokelson, R., Guenther, A., Greenberg, J., Blake, D., Artaxo, P.: TROFFEE (TROpical Forest and Fire Emissions Experiment): Investigating Emission, Chemistry, and Transport of Biogenic Volatile Organic Compounds in the Lower Atmosphere over Amazonia. J. Geophys. Res., 112, (D18), D18302, 2007.

Kirkman, G. A., Gut, A., Ammann, C., Gatti, L. V, Cordova, A. M., Moura, M. A. L., Meixner, F. X.: Surface exchange of nitric oxide, nitrogen dioxide, and ozone at a cattle pasture in Rondônia, Brazil, J. Geophys. Res., 107(D20), 8083, 2002.

Kvalevag M. M., Myhre, G.: The effect of carbon-nitrogen coupling on the reduced land carbon sink caused by tropospheric ozone, Geophys. Res. Letters, 40, 1-5, 2013.

Lamarque, J.-F., et al.: Historical (1850–2000) gridded anthropogenic and biomass burning emissions of reactive gases and aerosols: Methodology and application, Atmos. Chem. Phys., 10, 7017–7039, 2010.

Le Quéré, C. M. R., Raupach, J. G., Canadell, G. Marland et al.: Trends in the sources and sinks of carbon dioxide, Nature Geosciences, 2, 2009.

Lippmann, M.: Health effects of tropospheric ozone: review of recent research findings and their implications to ambient air quality standards, J. Exp. An. Environ. Epid., 3(1), 103-129, 1993.

776

777 Lloyd. J., Kolle, O., Fritsch, H., de Freitas, S. R., Dias, M. A. F. Silva, Artaxo, P., Nobre, A. D., de
778 Araujo, A. C., Kruijt, B., Sogacheva, L., Fisch, G., Thielmann, A., Kuhn, U., Andreae, M. O.: An
779 airborne regional carbon balance for Central Amazonia, Biogeosciences 4 (5): 759-768, 2007.

780

781 Logan, J., Megretskaia, I., Miller, A., Tiao, G., Choi, D., Zhang, L., Stolarski, R., Labow, G.,
782 Hollandsworth, S., Bodeker, G., Claude, H., De Muer, D., Kerr, J., Tarasick, D., Oltmans, S.,
783 Johnson, B., Schmidlin, F., Staehelin, J., Viatte, P., and Uchino, O.: Trends in the vertical
784 distribution of ozone: A comparison of two analyses of ozonesonde data, J. Geophys. Res., 104,
785 26373–26399, doi:10.1029/1999JD900300, 1999.

786

787 Martin, S. T., Andreae, M. O., Althausen, D., Artaxo, P., Baars, H., Borrmann, S., Chen, Q.,
788 Farmer, D. K., Guenther, A., Gunthe, S. S., Jimenez, J. L., Karl, T., Longo, K., Manzi, A., Müller,
789 T., Pauliquevis, T., Petters, M. D., Prenni, A. J., Pöschl, U., Rizzo, L. V., Schneider, J., Smith, J. N.,
790 Swietlicki, E., Tota, J., Wang, J., Wiedensohler, A., and Zorn, S. R.: An overview of the
791 Amazonian Aerosol Characterization Experiment 2008 (AMAZE- 08), Atmos. Chem. Phys., 10,
792 11415-11438, 2010.

793

794 Martin, G. M., et al.: The HadGEM2 family of Met Office Unified Model Climate configurations,
795 Geosci. Model Dev., 4, 723–757, 2011.

796

797 O'Connor, F. M., Johnson, C. E., Morgenstern, O., Abraham, N. L., Braesicke, P., Dalvi, M.,
798 Folberth, G. A., Sanderson, M. G., Telford, A. Voulgarakis, P. J., Young, P. J., Zeng, G., Collins,
799 W. J. and Pyle, J. A.: Evaluation of the new UKCA climate-composition model – Part 2: The
800 Troposphere, Geosci. Model Dev., 7, 41-91, 2014.

801

802 Oliveira, P. H. F., Artaxo, P., Pires Jr, C., de Lucca, S., Procópio, A., Holben, B., Schafer, J.,
803 Cardoso, L. F., Wofsy, S. C., Rocha, H. R.: The effects of biomass burning aerosols and clouds on
804 the CO_2 flux in Amazonia, Tellus Series B-Chemical and Physical Meteorology, 59B, (3) 338–349,
805 2007.
806
807 Olson, R. J., Scurlock, J. M. O., Prince, S. D., Zheng, D. L. and Johnson, K. R. (eds.). 2001. NPP
808 Multi-Biome: NPP and Driver Data for Ecosystem Model-Data Intercomparison
809
810 Ometto, J. P., Nobre, A. D., Rocha, H., Artaxo, P., Martinelli, L.: Amazônia and the Modern
811 Carbon Cycle: Lessons Learned. Oecologia, 143, 4, 483-500, 2005.
812
813 Pacifico, F., et al.: Evaluation of a photosynthesis-based biogenic isoprene emission scheme in
814 JULES and simulation of isoprene emissions under present-day climate conditions, Atmos. Chem.
815 Phys., 11, 4371–4389, 2011.
816
817 Pacifico, F., Folberth, G. A., Jones, C. D., Harrison, S. P. and Collins, W. J.: Sensitivity of biogenic
818 isoprene emissions to past, present, and future environmental conditions and implications_for
819 atmospheric chemistry, J. Geophys. Res., 117, D22302, 2012.
820
821 Palmer, J. R., and Totterdell, I. J.: Production and export in a Global Ocean Ecosystem Model,
822 Deep Sea Res., Part I, 48, 1169–1198, 2001.
823
824 Prentice, I. C. , Bondeau A., Cramer W., et al . 2007. Dynamic global vegetation modeling:
825 quantifying terrestrial ecosystem responses to large-scale environmental change. In: Canadell JG,
826 Pataki DE, Pitelka LF, eds. Terrestrial ecosystems in a changing world. IGBP Series. Berlin:
827 Springer, 175 – 192.

828

829 Price, C., and Rind, D.: A simple lightning parameterization for calculating global lightning
830 distributions, J. Geophys. Res., 97, 9919-9933, 1992.

831

832 Price, C., and Rind, D.: Modeling global lightning distributions in a general circulation model,
833 Mon. Weather Rev., 122, 1994.

834

835 Riahi, K., Gruebler, A. and Nakicenovic, N.: Scenarios of long-term socio-economic and
836 environmental development under climate stabilization, Technol. Forecast. Soc. Change, 74(7),
837 887–935, 2007.

838

839 Rich, S.: Ozone damage to plants, Ann. Rev. Phytopathol., 2, 253-266, 1964.

840

841 Rizzo, L. V., Artaxo, P., Muller, T., Wiedensohler, A., Paixao, M., Cirino, G. G., Arana, A.,
842 Swietlicki, E., Roldin, P., Fors, E. O., Wiedemann, K. T., Leal, L. S. M. and Kulmala, M.: Long
843 term measurements of aerosol optical properties at a primary forest site in Amazonia, Atmos.
844 Chem. Phys., 13, 2391–2413, 2013.

845

846 Rummel, U., Ammann, C., Kirkman, G. A., Moura, M. A. L., Foken, T., Andreae, M. O., and
847 Meixner, F. X.: Seasonal variation of ozone deposition to a tropical rain forest in southwest
848 Amazonia, Atmos. Chem. Phys., 7, 5415–5435, 2007.

849

850 Seinfeld, J. H., Pandis, S. N.,: Atmospheric Chemistry and Physics: from Air Pollution to Climate
851 Change. J. Wiley, New York, 1998.

852

853 Sierra, C. A., Harmon, M. E., Moreno, F. H., Orrego, S. A., Del Valle, J. I.: Spatial and temporal
854 variability of net ecosystem production in a tropical forest: testing the hypothesis of a significant
855 carbon sink. Glob. Change Biol., 13, 838–853, 2007.
856
857 Sigler, J. M., Fuentes, J. D., Heitz, R. C., Garstang, M., and Fisch, G.: Ozone dynamics and
858 deposition processes at a deforested site in the Amazon basin, Ambio, 31(1), 21-7, 2002.
859
860 Sitch, S., Cox, P. M., Collins, W. J., Huntingford, C.,: Indirect radiative forcing of climate change
861 through ozone effects on the land-carbon sink, Nature, 448, 791-95, 2007.
862
863 Stroud, C., Makar, P., Karl, T., Guenther, A., Geron, C., Turnipseed, A., Nemitz, E., Baker, B.,
864 Potosnak, M., and Fuentes, J. D., Role of canopy-scale photochemistry in modifying biogenic-
865 atmosphere exchange of reactive terpene species: Results from the CELTIC field study, J. Geophys.
866 Res., 110(D17303), doi:10.1029/2005JD005775, 2005.
867
868 Taylor, J. A., Lloyd, J.: Sources and sinks of atmospheric CO_2. Australian Journal of Botany, 40, 4-
869 5, 407-418, 1992.
870
871 Taylor, K. E., Stouffer, R., J. and Meehl, G. A.: An Overview of CMIP5 and the Experiment
872 Design, B. Am. Meteorol. Soc., 93.4, 2012.
873
874 Thompson et al. (2003a, b) Thompson, A., Witte, J., McPeters, R., Oltmans, S., Schmidlin, F.,
875 Logan, J., Fujiwara, M., Kirchhoff, V., Posny, F., Coetzee, G., Hoegger, B., Kawakami, S., Ogawa,
876 T., Johnson, B., Vomel, H., and Labow, G.: Southern Hemisphere Additional Ozonesondes
877 (SHADOZ) 1998–2000 tropical ozone climatology – 1. Comparison with Total Ozone Mapping

878 Spectrometer (TOMS) and ground-based measurements, J. Geophys. Res., 108, 8238,
879 doi:10.1029/2001JD000967, D2, 2003a.
880
881 Thompson, A., Witte, J., Oltmans, S., Schmidlin, F., Logan, J., Fujiwara, M., Kirchhoff, V., Posny,
882 F., Coetzee, G., Hoegger, B., Kawakami, S., Ogawa, T., Fortuin, J., and Kelder, H.: Southern
883 Hemisphere Additional Ozonesondes (SHADOZ) 1998–2000 tropical ozone climatology – 2.
884 Tropospheric variability and the zonal wave-one, J. Geophys. Res., 108, 8241,
885 doi:10.1029/2002JD002241, D2, 2003b.
886
887 Thompson, T. M., and Selin. N. E.: Influence of air quality model resolution on uncertainty
888 associated with health impacts, Atmos. Chem. Phys., 12, 9753-9762, 2012.
889
890 Tie, X., Brasseur, G. and Ying, Z.: Impact of model resolution on chemical ozone formation in
891 Mexico City: application of the WRF-Chem model, Atmos. Chem. Phys., 10, 8983-8995, 2010.
892
893 van der Werf, G. R., Randerson, J. T., Giglio, L., Collatz, G. J., Kasibhatla, P. S., and Arellano, A.
894 F.: Interannual variability in global biomass burning emissions from 1997 to 2004, Atmos. Chem.
895 Phys., 6, 3423–3441, 2006.
896
897 van der Werf et al.: Global fire emissions and the contribution of deforestation, savanna,
898 forest, agricultural, and peat fires (1997–2009), Atmos. Chem. Phys., 10, 11707–11735, 2010.
899
900 Valari, M., and Menut, L.: Does an increase in air quality Models' resolution bring surface ozone
901 concentrations closer to reality?, J. Atm. Oceanic Tech., 25, 2008.
902
903 Wesely, M. L.: Parameterization of surface resistances to gaseous dry deposition in regional-scale

numerical models, Atmos. Environ., 23, 1293–1304, 1989.

Yienger, J. J., and Levy II, H.: Global inventory of soil-biogenic NOx emissions, J. Geophys. Res., 100, 11,447–11,464, 1995.

908

909 Figures

910

911 1. Comparison of measured (dots) and simulated (stars) monthly averaged diurnal cycle of
912 surface O_3 mixing ratios at the Porto Velho site, including measured day-to-day variability (grey
913 lines) and standard deviation (dashed lines) for the model results. The measurements have an
914 uncertainty of 4%.

915

916 2. Comparison of measured (dots) and simulated (stars) monthly averaged diurnal cycle of
917 surface O_3 mixing ratios at the ZF2 site in the Cuieiras forest reserve, including measured day-to-
918 day variability (grey lines) and standard deviation (dashed lines) for the model results. The
919 measurements have an uncertainty of 4%. We show one of the two available years of observations.
920 Legend as in Figure 1.

921

922 3. Vegetation cover in HadGEM2 for the month of September. The red rectangle is our region
923 of analysis. The two sites used in the model evaluation (the sites of Porto Velho and ZF2 site in the
924 Cuieiras forest reserve) are also marked.

925

926 4. Monthly average surface O_3 mixing ratio simulated with HadGEM2 for the month of
927 September (average over 8 years of simulations).

928

929 5. Clockwise from the top-left: (a) Simulated monthly surface O_3 mixing ratios; (b) Simulated
930 monthly total NPP; (c) Simulated monthly variation in total NPP. The plots show the results for the
931 control simulation (i.e. using the decadal mean biomass burning emissions from Lamarque et al.
932 (2010) centered on year 2000; 2000 BB emissions) and the various experiments with increased (+)

933 or decreased (-) biomass burning emissions over South America by 20, 40, 60, 80 and 100%. All
934 data are averaged over the region of analysis for 8 years of simulations.
935
936 6. From the left: simulated variation in surface O_3 mixing ratios and NPP over the region of
937 analysis for the months of August, September and October.
938
939 7. Probability density function (histogram) of the variation in NPP for the same months. The
940 plots show the variation between the experiments with South American biomass burning
941 increased/decreased by 40, 60 and 100% and the control simulation.

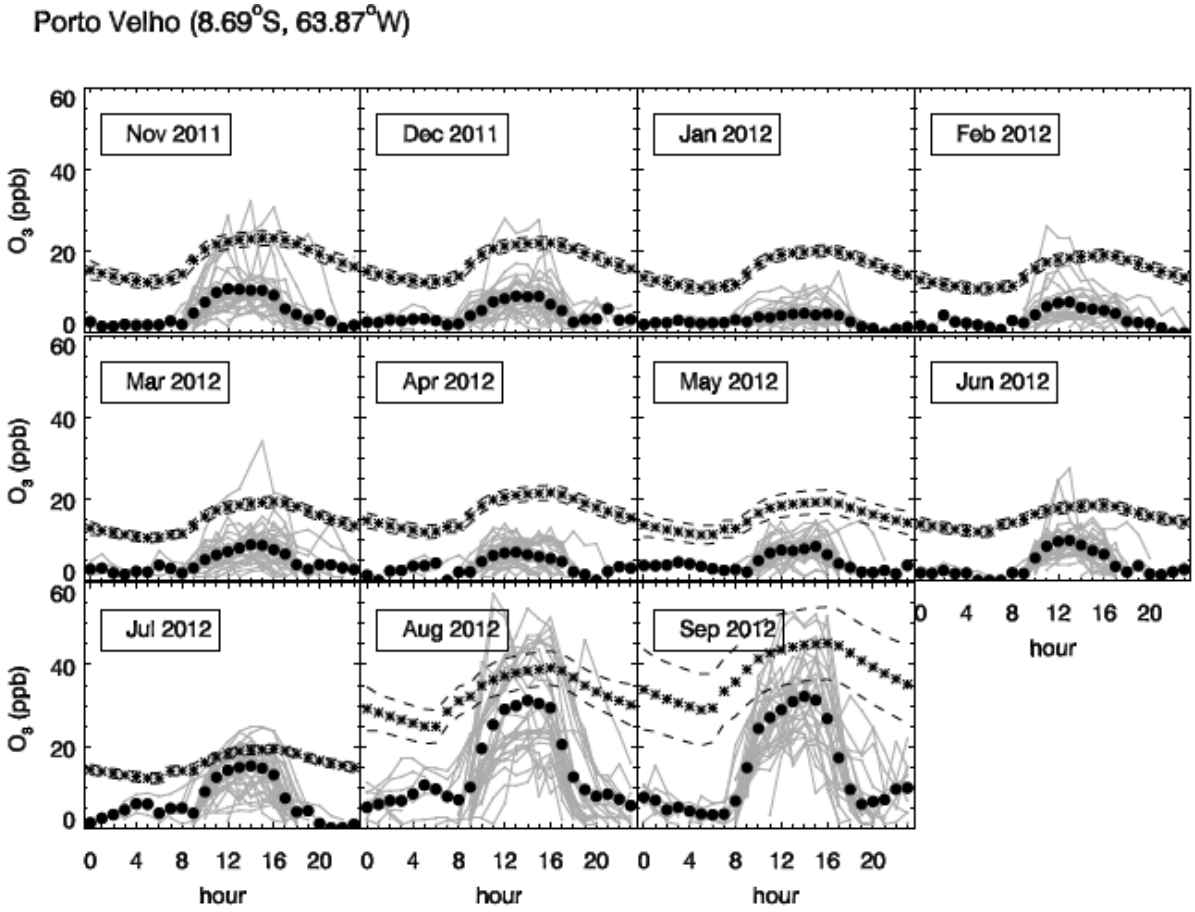

942

943 Figure 1

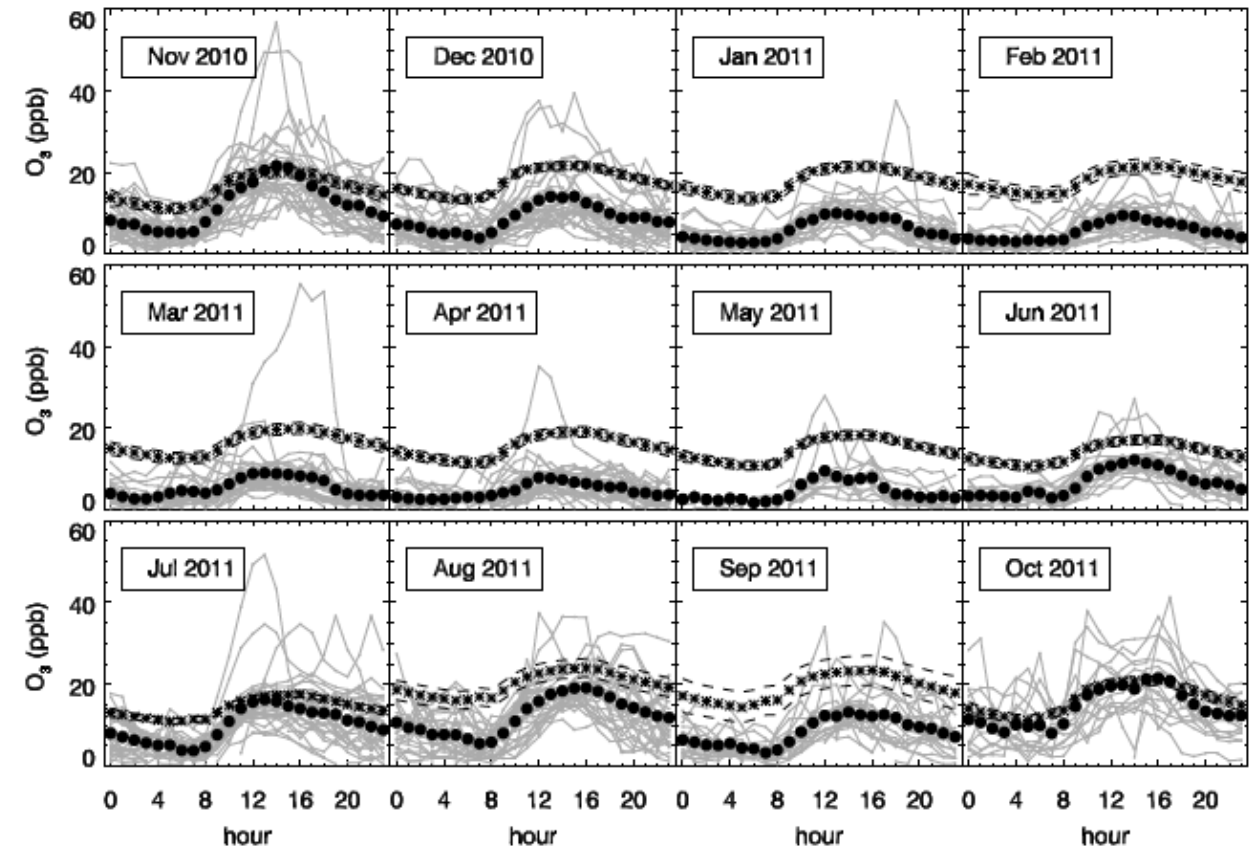

944

945 Figure 2

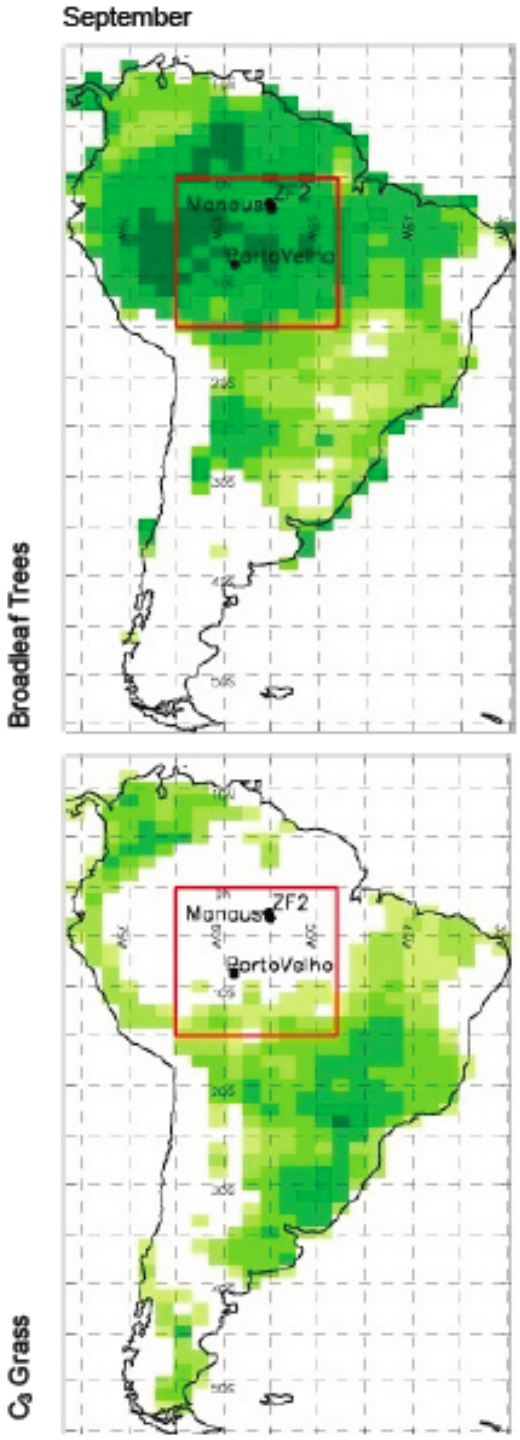

946

947 Figure 3

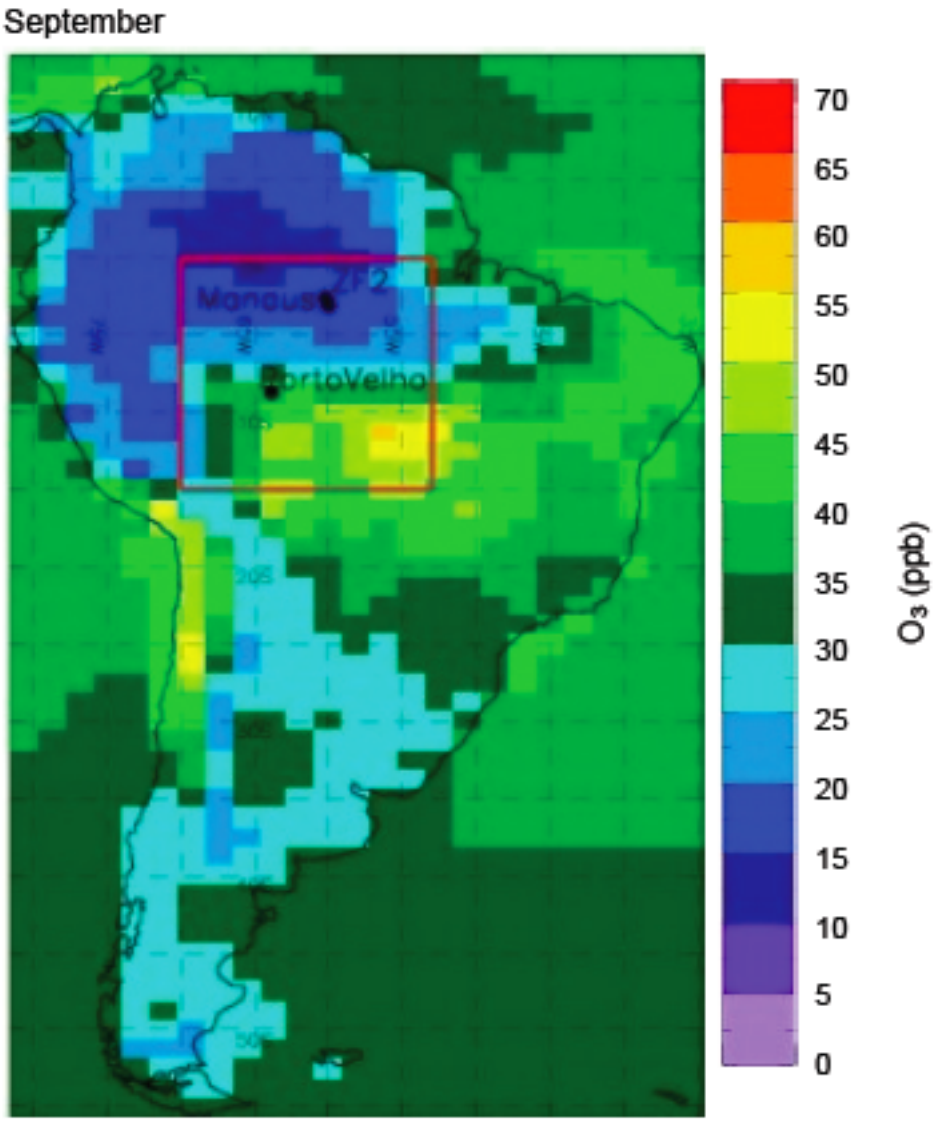

948

949 Figure 4

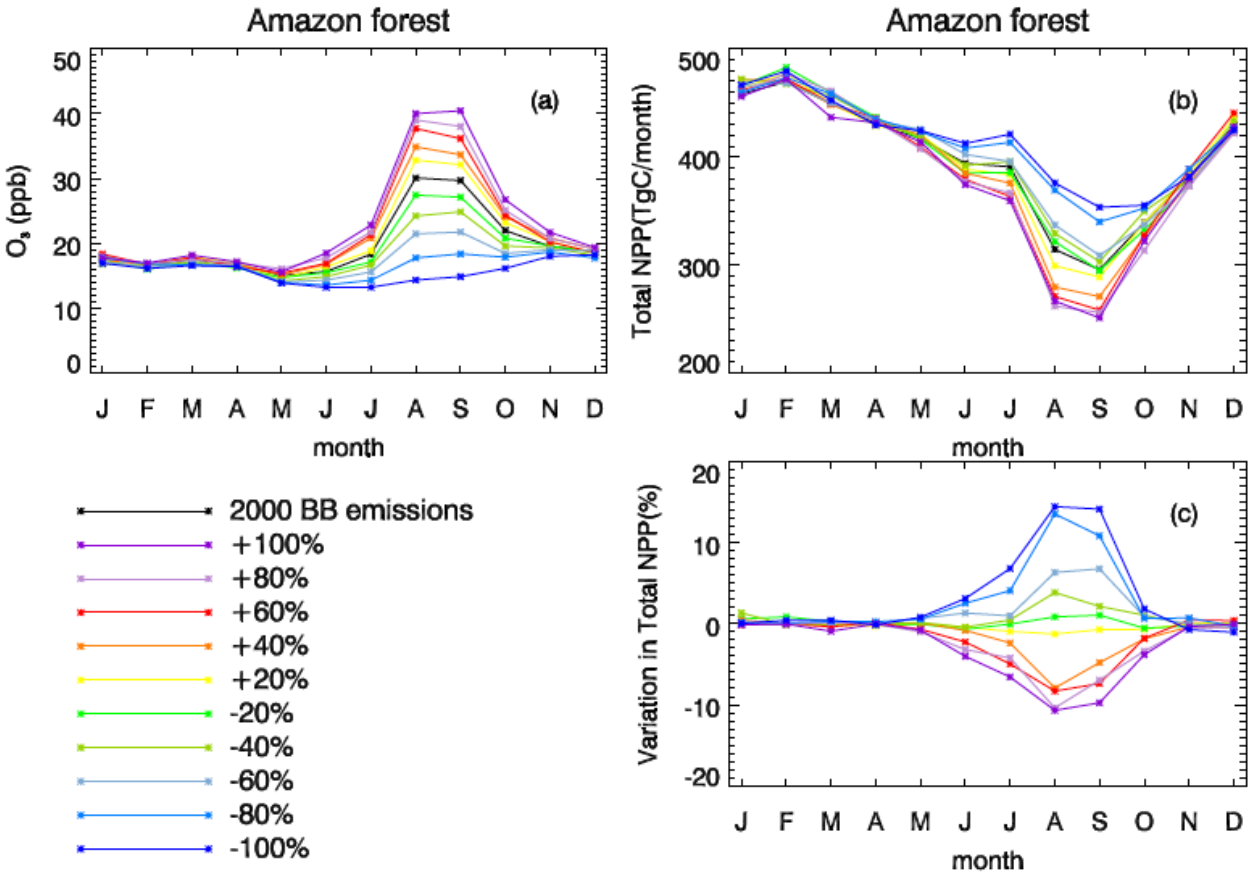

950

951 Figure 5

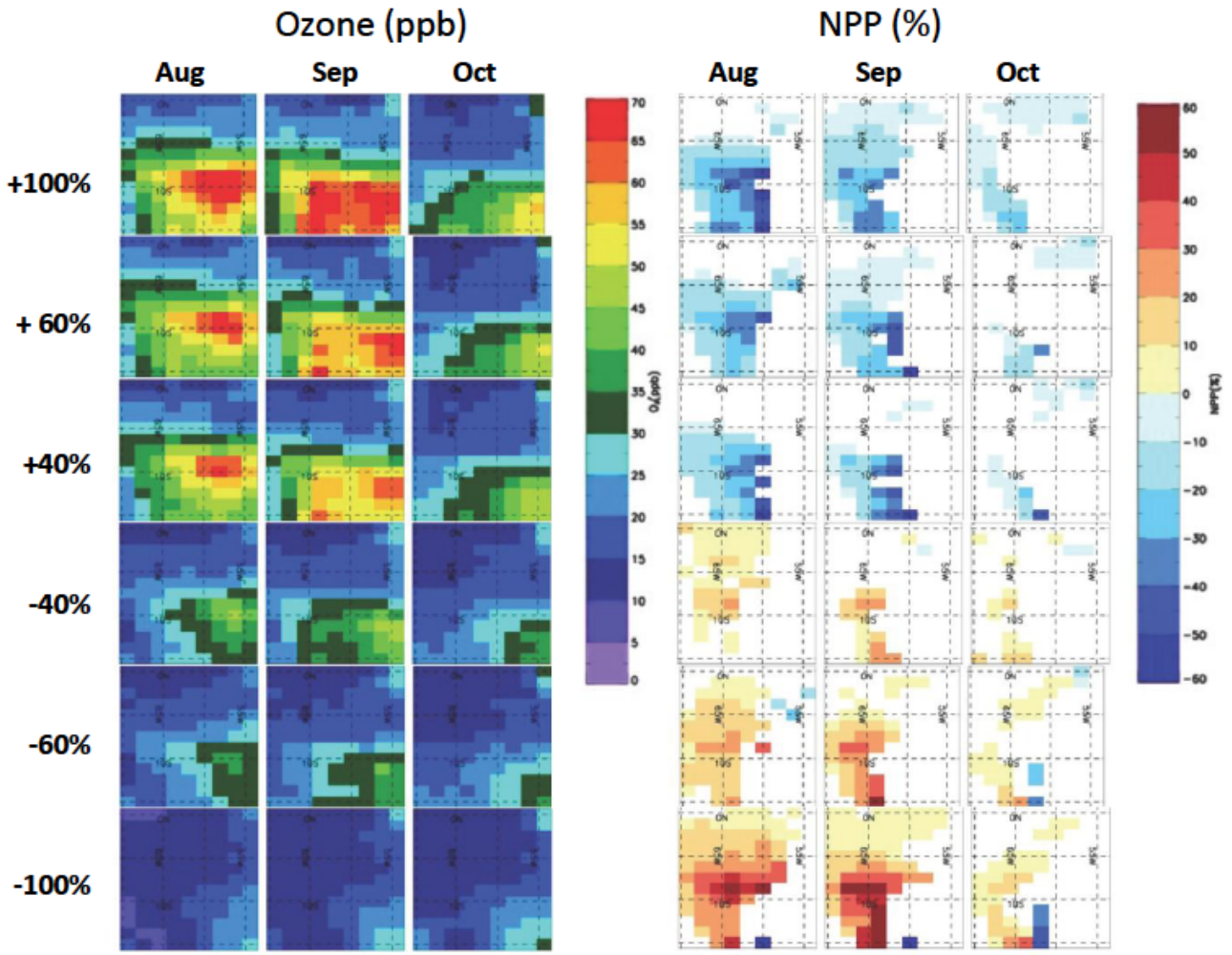

952

953 Figure 6

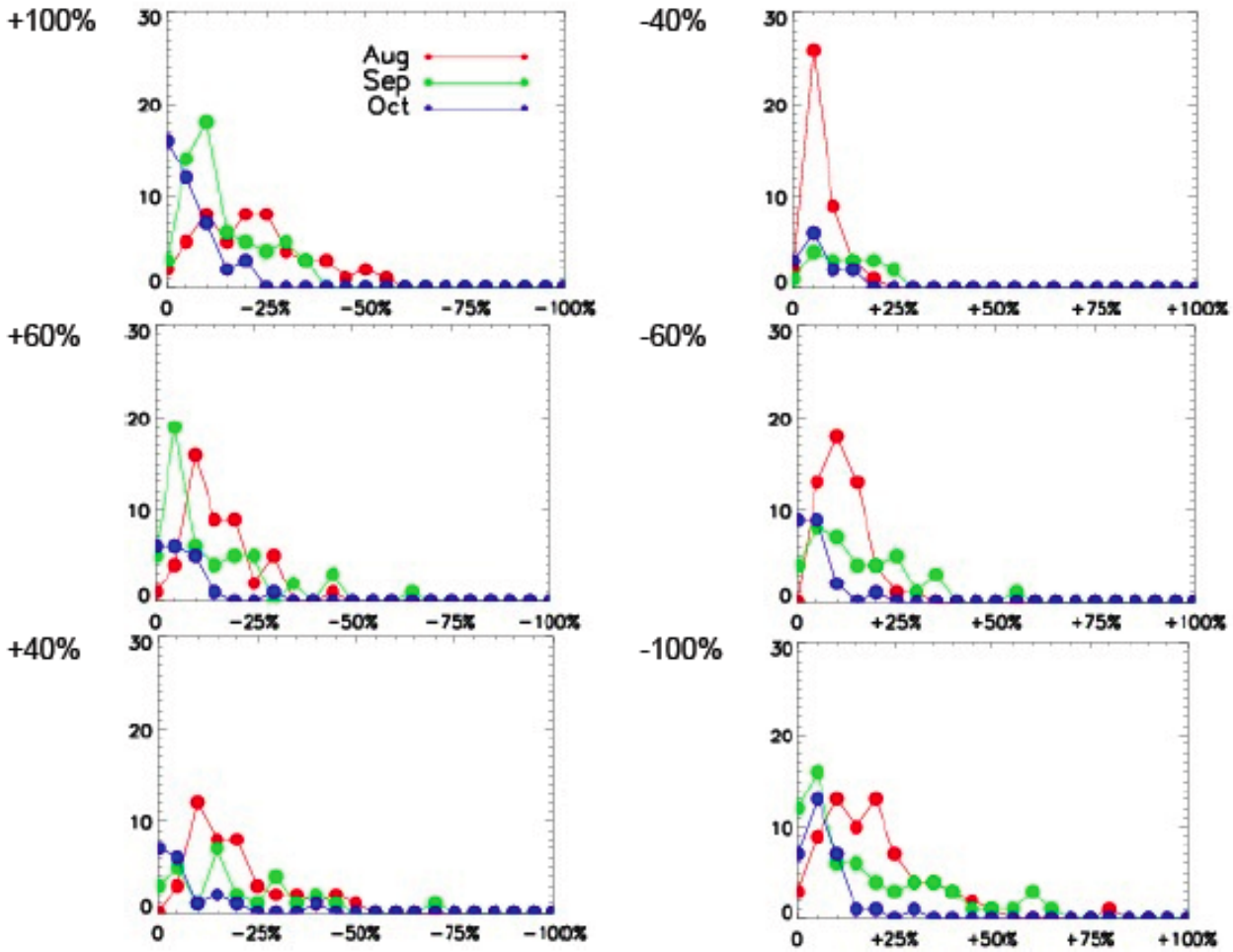

954

955 Figure 7

956